IJC Heart & Vasculature 40 (2022) 101028

Contents lists available at ScienceDirect

IJC Heart & Vasculature

journal homepage: www.sciencedirect.com/journal/ijc-heart-and-vasculature

Mechanical dispersion combined with global longitudinal strain estimated by three dimensional speckle tracking in patients with ST elevation myocardial infarction

Noriaki Iwahashi [a,*], Jin Kirigaya [a], Masaomi Gohbara [a], Takeru Abe [b], Mutsuo Horii [a], Yohei Hanajima [a], Noriko Toya [c], Hironori Takahashi [a], Hidekuni Kirigaya [a], Yugo Minamimoto [a], Yuichiro Kimura [a], Kozo Okada [a], Yasushi Matsuzawa [a], Kiyoshi Hibi [a], Masami Kosuge [a], Toshiaki Ebina [a], Kouichi Tamura [d], Kazuo Kimura [a]

[a] Division of Cardiology, Yokohama City University Medical Center, Yokohama, Japan
[b] Department of Emergency Medicine, Yokohama City University Medical Center, Yokohama, Japan
[c] Department of Radiology, Yokohama City University Medical Center, Yokohama, Japan
[d] Department of Medical Science and Cardiorenal Medicine, Yokohama City University Graduate School of Medicine, Yokohama, Japan

ARTICLE INFO

Keywords:
STEMI
Speckle tracking
Three dimensional echocardiography
Mechanical dispersion
Prognosis

ABSTRACT

Background: The role of left ventricular (LV) mechanical dispersion estimated after an ST elevation acute myocardial infarction (STEMI) remains unclear.

Methods: The study participants were 208 consecutive patients (152 men, age = 72 years) presenting with STEMI for the first time who underwent primary percutaneous coronary intervention (PCI) within 12 h of STEMI onset. Within 48 h of PCI (mean = 24 h), 2D and 3D speckle-tracking echocardiography were performed. The global longitudinal strain (GLS) was calculated using 3D (3D-GLS) and 2D (2D-GLS) speckle tracking. Mechanical dispersion was defined using the standard deviation (SD) of the time to regional peak longitudinal strain (LS) for all 16 segments for both 2D-STE and 3D-STE (2D-LS-SD, 3D-LS-SD). Infarct size was estimated by Tc99m-sestamibi as the total area of < 50% of the uptake area at 2 weeks. The patients were followed up for a longer period of time (median118months) and checked for major adverse cardiac events (MACE: cardiac death, heart failure).

Results: During follow-up, 55 patients experienced MACE. The cut-off values were determined using receiver operating characteristic curves. The multivariate analysis revealed that a 3D-LS-SD > 56.7 ms was a significant predictor of MACEs (hazard ratio = 1.991, 95% confidence interval 1.033–3.613, p = 0.03), but 2D-LS-SD > 58.1 ms was not an independent predictor of MACEs (hazard ratio = 1.577, 95% confidence interval 0.815–3.042, p = 0.1). Furthermore, the combination of 3D-GLS and 3D-LS-SD had accurate predictability for MACE, as shown by the Kaplan-Meier curves (log rank, $\chi^2 = 94.1$, $p < 0.0001$).

Conclusions: LV mechanical dispersion besides 3D-GLS assessed by 3D-STE immediately after PCI can predict long-term prognosis.

1. Introduction

Left ventricular (LV) mechanical dispersion has a deleterious effect on hemodynamic function and prognosis in patients with heart failure (HF). [1] In fact, LV mechanical dispersion has been reported as an important factor even for acute myocardial infarction (AMI) [2 3], as well the other cardiovascular diseases.[4] Previous studies have demonstrated the relationships between the factors such as preexisting hypertension, infarct size, and anterior location of the infarct and the occurrence of LV remodeling after AMI.[5] Infarct size greatly impacts

Abbreviations: 2D, two-dimensional; 3D, three-dimensional; AMI, acute myocardial infarction; CI, confidence interval; GLS, global longitudinal strain; HF, heart failure; IQR, interquartile range; LV, left ventricular; STEMI, ST-segment elevation myocardial infarction.

* Corresponding author at: Division of Cardiology, Yokohama City University Medical Center, 4-57 Urafune-cho, Minami-ku, Yokohama 232-0024, Japan.
E-mail address: wsnorikun@yahoo.co.jp (N. Iwahashi).

https://doi.org/10.1016/j.ijcha.2022.101028
Received 3 December 2021; Received in revised form 27 March 2022; Accepted 3 April 2022

on LV synchronicity, therefore we think that mechanical dispersion reveals one type of LV function impairment.

Two-dimensional speckle tracking (2D-ST) strain echocardiography enables the evaluation of mechanical dispersion immediately after AMI that can lead to LV remodeling[6] and prognosis.[7,8 9] Recently real time three-dimensional echocardiography (RT3DE) has enabled the accurate evaluation of wall motion abnormalities.[10] Thus, we have reported that 3D-global longitudinal strain (3D-GLS) determination is clinically useful in patients with STEMI because it can predict LV remodeling and the short and long-term prognosis.[11,12] For this reason, we anticipated that mechanical dispersion could also be evaluated by 3D-STE because mechanical dispersion may be evaluated as a 3D structure.

Therefore, the clinical usefulness of 3D-STE and 2D-STE in estimating LV mechanical dispersion in patients with STEMI for the first time was compared. The patients were followed up for a longer period of time and the prognostic usefulness of determining mechanical dispersion using 3D-STE was assessed.

2. Methods

2.1. Patients

A total of 259 STEMI patients were assessed between April 2009 and August 2012 at Yokohama City University Medical Center, Yokohama, Japan. Patients who underwent reperfusion therapy using percutaneous coronary intervention (PCI) within 12 h after the onset of STEMI symptoms were enrolled. STEMI was defined as (1) typical chest pain lasting $>$ 30 min, (2) ST-segment elevation $>$ 0.1 mV in two contiguous leads on initial ECG, and (3) elevation of creatinine phosphokinase (CPK) level to twice the upper limit of the normal range. Supplementary Fig. 1 shows the protocol used for patient selection. The inclusion criteria were as follows: (1) age $>$ 20 years and (2) successful revascularization of the infarct-related artery using primary PCI within 12 h of the onset of chest pain. The exclusion criteria were as follows: (1) previous myocardial infarction (n = 12), (2) significant valvular heart disease (n = 6), (3) chronic atrial fibrillation (n = 11), (4) inadequate myocardial tracking by 2D-STE or 3D-STE due to fair image quality or volume rate (n = 20) heamodialysis (n = 2). The final study population comprised of 208 patients who underwent echocardiography approximately 24 h after admission (within 48 h). Reperfusion time was defined as the time from symptom onset to reperfusion (TIMI grade 2). Each patient underwent ^{99m}Tc–sestamibi single-photon emission computed tomography (SPECT) at 7–14 days after PCI to estimate the final infarct size and function. Patients were administered an intravenous injection of 16 mCi (600 MBq) ^{99m}Tc-sestamibi, and SPECT was performed 1 h after injection of the radioactive agent. Infarct size was defined as $<$ 50% of uptake area calculated by an experienced radioisotope technician (N.T.). The highest levels of creatinine and plasma brain natriuretic peptide (BNP) during hospitalization were also measured, and the estimated glomerular filtration rate (eGFR) was calculated. The CPK level and myocardial band (MB) were first determined on admission at 3 h intervals during the first 24 h, at 6 h intervals for the next 2 days, and then daily until discharge; the values were used to determine the maximum CPK/MB level. All the patients underwent exercise test such as 200 M course test or master stress test during the initial hospitalization, and discharged hospital if the test was negative. The patients were followed up for a median of 118 months (interquartile range [IQR], 96–129 months; follow-up rate = 100%) on regular visits to their attending physicians or by telephone interviews. The primary endpoint was any occurrence of a major adverse cardiac event (MACE: incidence of cardiac death and HF). The secondary endpoint was all-cause mortality. HF was defined according to the Framingham criteria for congestive HF with hospitalization. Telephone contact with patients, physicians, and the next of kin was made if the patients had been treated at another hospital. The Institutional Review Board waived the requirement for individual informed consent according to the "opt-out" principle in a retrospective study. Patients could opt out of the database if they wished. The study protocol was approved by the ethics committee of our institute and conducted according to the provisions of the Declaration of Helsinki (UMIN000041995).

2.2. Echocardiography

Both 2D and 3D echocardiography were performed using iE33 (Philips Medical Systems, Andover, MA, USA) by an experienced cardiologist (N.I.). Patients were examined in the left lateral or supine position based on examinations of precordial 2D and 3D echocardiographic images. LV volumes (end-diastolic volume [EDV], end-systolic volume [ESV]) and ejection fraction (EF) were calculated using 3D echocardiography. The left atrial (LA) volume was calculated using the area length method. The mitral inflow peak early velocity (E)/mitral annular peak early velocity (e′) was obtained and the E/e′ ratio was calculated. The severity of mitral regurgitation was visually assessed. Based on previous guidelines, 3D full-volume data were acquired from the apical view while the patients held their breath using a matrix array transducer (X3-1, Philips Medical Systems)[13]. To ensure the inclusion of the entire LV region within the pyramidal scan volume with a high volume rate, data sets from four cardiac cycles were acquired using the wide-angle mode, wherein multiple wedge-shaped subvolumes were acquired with electrocardiographic gating for at least 5–7-second single breath holds (they were stitched data).

2.3. 2D-STE

2D-STE was performed using vendor-independent 2D speckle-tracking software (2D Cardiac Performance Analysis Ver 1.3, TomTec Imaging Systems, Germany) based on the appropriate method by two experienced investigators (N.I. and J.K.)[14]. The longitudinal strain was measured by manual tracing of the endocardial border in three apical views. After a frame-by-frame speckle-tracking analysis of the LV endocardium that averaged more than two cardiac cycles, the software provided regional strain curves of six segments in each view, from which the peak regional strain value was calculated. GLS was calculated as the peak strain value from the average of 16 segmental strain curves (2D-GLS). The time to regional peak longitudinal strain (LS) was measured, and the standard deviation (SD) between all 16 segments (2D-LS-SD) was used to measure the mechanical dispersion of 2D-STE. The adequacy of tracking was visually verified, and if tracking was not considered optimal, the endocardial border was manually adjusted.

2.4. 3D-STE

Three-dimensional strain measurements of the LV were performed using the 3D-STE. Patients with a volume rate $>$ 25/sec were determined to analyze mechanical dispersion. Three-dimensional full-volume datasets (stitched data) were analyzed using vendor-independent 3D speckle-tracking software (4D LV Analysis, version 3.1, TomTec Imaging Systems, Germany) by two experienced investigators (N.I. and J.K.). After importing 3D full-volume data sets, the apical 4-chamber, 2-chamber, and 3-chamberviews and three short-axis views at the end-diastolic period were automatically extracted. Apical views were identified to select the point of the apex and the center of the mitral annular line connecting both sides of the mitral annulus with the LV long-axis dimensions, after which the 3D endocardial surface was traced. If this was not optimal, manual adjustments of the endocardial surface were performed. This procedure was performed at the end-systolic frame. Subsequently, the software performed 3D speckle-tracking analysis throughout the cardiac cycle. For the 3D strain analysis, the LV was divided into 16 segments. The software provided segmental LS time curves, from which peak global strain and average peak strain at three LV levels (basal, midventricular, and apical) were determined (3D-GLS)

[15]. The time to regional peak LS was measured, and the SD between all 16 segments (3D-LS-SD) was used to measure the mechanical dispersion of 3D-STE. When tracking was not good, the endocardial surface was manually retraced. If tracking was still inaccurate, participants were excluded from the analysis. Supplementary Fig. 2 shows a representative case of the 3D speckle-tracking analysis. The left panels show the endocardial tracking, whereas the right panels show the LS curves. The upper right panel (A) shows the LS curves with no MACE. The patient's 3D-GLS was −12.5, his 3D-LS-SD was 35.5 ms, and he had no significant mechanical dispersion. The lower right panel shows the LS curves with a MACE. The patient's 3D-GLS was −12.7, his 3D-LS-SD was 58.0 ms, and he had mechanical dispersion.

2.5. Reproducibility

Intraobserver and interobserver (N.I. and J.K.) variabilities in 2D-STE and 3D-STE measurements were assessed in 20 randomly selected participants in this study, and the agreement between 3D-GLS and 3D-LS-SD was assessed using Bland-Altman analysis[16] with a predefined accuracy set as 95% limits of agreement ± 2SD.

2.6. Statistical analysis

Continuous variables were evaluated using Kolmogorov-Smirnov tests for a normal distribution. For uniformity, summary statistics for all continuous variables are presented as medians with IQRs. Categorical variables were summarized as frequencies and percentages. We used the Student's *t*-test or Mann-Whitney *U* test for continuous variables and the chi-squared test for categorical variables to compare between a patient group with the occurrence of MACE and a group without MACE. Interobserver and intraobserver reproducibility were assessed in 20 randomly selected patients using the Bland-Altman analysis[16]. To determine the optimal threshold of 2D- and 3D-STE (GLS and LS-SD) for the prediction of endpoints, receiver operating characteristic curve (ROC) analysis was applied. We compared area under the curves (AUCs) of 3D and 2D-STE using DeLong's Method. We calculated Kaplan-Meier curves for MACE of the four groups categorized based on the cut-off values of 3D-GLS and 3D-LS-SD, as determined by ROC curves. The log-rank test was used to evaluate differences among the groups. Next, to control for the effects of confounding factors, we adopted two Cox proportional hazard models for the prediction of MACE with all independent variables using either 2D or 3D indices. Cut-off values of 2D, 3D-STE or 3D-GLS from the ROC analysis above were also included in these models. We divided the patients according to the value of 3D-GLS (median value = -12.4%). For all tests, a two-sided p value < 0.05 was considered statistically significant. The correlations and Bland-Altman plot analyses[16] were calculated.

Statistical analyses were performed using JMP Pro 15 software (SAS Institute, Inc., Cary, NC, USA).

3. Results

3.1. Baseline data of the study population

Table 1 shows the characteristics of the patients and their categorization according to the presence of MACE. Significant differences were detected between patients with MACE and without MACE in terms of systolic blood pressure, multivessel disease, BNP, eGFR, QRS duration at the CCU, QRS duration at 24 h, QRS duration at 2 weeks, LVESVI, LVEF, E/e', MR grade, 2D-GLS, 3D-GLS, 2D-LS-SD and 3D-LS-SD (Table 1). Significant relationships were detected between the LS-SD and QRS duration, infarct size, 3D-GLS, and E/e' (Supplementary Fig. 3). Supplementary table1 shows the data from the other indices.

Table 1
Patient characteristics according to the presence of the adverse cardiac events.

	MACE (+)		MACE (-)		*p*-value*
	n = 55		*n* = 153		
Patients background					
Age (years)	72	(63–78)	62	(55–73)	<0.0001
Sex male, n (%)	28	−67	124	−82	0.26
BSA (m^2)	1.67	(1.52–1.75)	1.72	(1.56–1.85)	0.07
sBP (mmHg)	103	(95–121)	110	(100–121)	0.04
dBP (mmHg)	60	(51–64)	60	(56–66)	0.3
HR (bpm)	76	(66–83)	72	(66–80)	0.18
Clinical indices					
Hypertension (yes)	36	−65	85	−56	0.21
Diabetes mellitus (yes)	13	–23	42	–23	0.56
Anterior MI (yes)	36	−66	71	−47	0.02
MVD, n (%)	30	−55	48	–32	0.002
Killip > 1	24	−44	33	–22	0.002
Reperfusion time, min	160	(108–275)	130	(95–209)	0.06
>360 min, n (%)	8	−14	19	−12	0.16
<120 min, n (%)	18	–32	64	−41	0.23
No reflow/ Slow flow, n (%)	9	−16	13	−8	0.11
Biochemical markers					
Admission BNP (pg/ml)	49.7	(26.7–189.7)	22.3	(9.9–58.3)	<0.0001
Maximum BNP (pg/ml)	219.5	(90.65–522.9)	69.4	(38.3–159.6)	<0.0001
eGFR (ml/min/ 1.73 m^2)	52.2	(44.0–64.9)	64.6	(55.3–79.5)	<0.0001
MIBI SPECT					
Infarct size	16.5	(0.5–53.6)	5	(0–25)	0.04
ECG					
QRS duration ER (msec)	96	(90–110)	98	(90–105)	0.42
QRS duration CCU (msec)	96	(90–103)	94	(88–100)	0.06
QRS duration 2 weeks (msec)	92	(85–105)	90	(85–98)	0.1
Echocardiography					
LVEDVI (ml/ m^2)	64.6	(51.9–77.7)	60.8	(47.6–72.3)	0.08
LVESVI (ml/ m^2)	32.4	(24.6–48.1)	26.6	(19.3–36.5)	0.007
LVEF (%)	45	(35–61)	53	(45–62)	0.03
LAVI (ml/m^2)	39	(31.3–51.5)	33.1	(26.8–44.1)	0.02
E/A	0.89	(0.68–1.31)	0.84	(0.68–1.1)	0.23
Dct (msec)	187	(155–256)	204	(173–253)	0.14
E/e'	15.3	(12.7–18.1)	11.9	(9.3–15)	<0.0001
MR≧Moderate	10	−17	7	−5	0.001
Speckle tracking					
2D-GLS (%)	−10	(-12.0 - −8.0)	−13.15	(-15.0- −12.0)	<0.0001
3D-GLS (%)	−8.8	(-10.8- −6.4)	−13.2	(-15.2- −11.6)	<0.0001
2D-LD-SD	65.9	(52.8–80.6)	52.8	(43.3–64.5)	<0.0001
3D-LD- SD	67.3	(41.7–85.1)	52.7	(41.4–63.9)	<0.0001

* *p*-values were for patients with MACE versus with MACE; MACE = major adverse cardiac events; BSA = body surface area; BP = blood pressure; HR = heart rate; MVD = multivessel disease; BNP = brain natriuretic peptide; eGFR = estimated glomerular filtration rate; MIBI = 99mTc methoxy-isobutyl-isonitril; SPECT = single photon emission computed tomography; EDV = end-diastolic volume; ESV = end-systolic volume; EF = ejection fraction; E = early diastolic wave velocity; A = late diastolic; Dct = deceleration time; e' = early diastolic velocity of mitral annulus; LAV = left atrial volume; MR = mitral regurgitation; 2D = 2 dimensional, 3D = 3 dimensional, GLS = global longitudinal strain, LS-SD = standard deviation of longitudinal strain

3.2. Long-term prognosis

During the follow-up period (118 months), 55 patients experienced MACE (21 cardiac deaths, 34 HF hospitalizations). Calculation of ROC curves to determine the appropriate cut-off values (Fig. 1) revealed values of −11.2 for 2D-GLS, 58.1 ms for 2D-LS-SD, −11.3 for 3D-GLS, and 56.7 ms for 3D-LS-SD. These ROC curves revealed significant differences between 2D-GLS and 3D-GLS(1-left), as well as between 2D-LS-SD and 3D-LS-SD(1-right), using DeLong's method. The 3D-GLS and 3D-LS-SD were stronger predictors of MACE than 2D-GLS and 2D = LS-SD, respectively.

Table 2 shows the univariate and Cox proportional hazards models used to predict MACE. The univariate comparisons revealed that age > 75 years, infarct size > 20%, 2D-GLS > -11.2, 2D-LS-SD > 58.1 ms, 3D-GLS > -11.3, and 3D-LS-SD > 56.7 ms were significant predictors. The Cox proportional hazards models with 2D strain indices identified age > 75 years and 2D-GLS > -11.2 as the independent predictors. The 3D strain indices showed that age > 75 years, 3D-GLS > -11.3, and 3D-LS-SD > 56.7 ms were independent predictors.

Fig. 2 show the Kaplan-Meier curves for the prediction of MACE by 3D-GLS = -11.3 (A) and 3D-LS-SD = 56.7 ms (B). These curves differed significantly in terms of the MACE occurrence. Fig. 2A shows the significant difference between patients with 3D-GLS < -11.3 and ≧-11.3 (Log rank, $\chi^2 = 87.0$, $p < 0.0001$). Fig. 2B shows the significant difference between the patients with 3D-LS-SD < 56.7 ms and ≧56.7 ms(log rank, $\chi^2 = 21.9$, $p < 0.0001$). Next, we divided them into four groups; Group A: 3D-GLS < -11.3 and 3D-LS-SD < 56.7 ms, Group B: 3D-GLS≧-11.3 and 3D-LS-SD < 56.7 ms, Group C: 3D-GLS < -11.3 and 3D-LS-SD≧56.7 ms, Group D: GLS≧-11.3 and 3D-LS-SD≧56.7 ms. Fig. 2C shows the significant differences among 4 groups (log rank, $\chi^2 = 94.1$, $p < 0.0001$). Calculation of Kaplan-Meier curves for the four groups(C) indicated that the combination of the 3D-GLS and 3D-LS-SD was the strongest prognosticator. Fig. 3 shows the 3D-GLS and 3D-LS-SD plots, with the red plot indicating the patients with MACE and the blue plot indicating the patients without MACE. There were significant differences in the frequency of MACE among the four groups (Pearson's, $\chi^2 = 101.1$, $p < 0.0001$). Table3 shows the comparison of the hazard risk among the four groups. A higher incidence was observed in Group D than that in the other groups. Supplementary Table 2 shows the results of the Cox hazard analysis using age, paroxysmal atrial fibrillation, ventricular tachycardia/ventricular fibrillation and CRP, of which age was the strongest.

3.3. Reproducibility

The intraobserver variabilities for the 3D strain were 9.3% for 3D-GLS and 8.4% for 3D-LS-SD. The corresponding inter-observer variabilities for 3D-GLS and 3D-LS-SD were 9.8% and 9.6%, respectively. Bland-Altman plot analysis revealed a bias of 0.298 for 3D-GLS calculated by two observers with 95% limits of agreement ranging from −0.629 to −0.617. A similar result was also observed following the 3D-LS-SD analysis, which revealed a bias of 1.832, as calculated by two observers, with 95% limits of agreement ranging from −3.224 to 4.399.

4. Discussion

The main findings of this study were that the GLS and mechanical dispersion calculated by 3D-STE were significant predictors following the onset of STEMI. The predictive value of the combination of 3D-GLS and 3D-LS-SD was excellent, according to the Kaplan-Meier curve analysis. Therefore, 3D-STE enables the simultaneous measurement of GLS and mechanical dispersion, while also enabling the prediction of prognosis after STEMI. Mechanical dispersion by 3D-STE was especially useful in patients with preserved 3D-GLS.

4.1. Novelty of the current study

Our study differs from existing studies through the use of different approaches. First, 3D echocardiography was performed 24 h after the onset of STEMI. Second, the effects of confounding factors were reduced by including only those patients who had undergone their first STEMI with reperfusion within 12 h of symptom onset. A third difference was that a strain analysis was performed using vendor-independent software. Furthermore, cardiac function was analyzed and infarct size was estimated using SPECT. The patients in this study were also followed up for a median of approximately 10 years.

4.2. Mechanical dispersion for STEMI

Mechanical dispersion may decrease both ventricular contractile efficiency and cardiac output[17], and progressive LV remodeling is one recognized mechanism that mediates prognosis [18]. Our results confirm the findings of recent reports on the clinical usefulness of LV dispersion using 2D-STE [9]. Previous studies have suggested that electrical dispersion due to RV pacing is associated with progressive LV enlargement, worsening LV systolic function, and LA enlargement.[19] Abnormal patterns of contraction and myocardial stretch caused by LV dispersion are likely to increase mechanical loading and myocardial

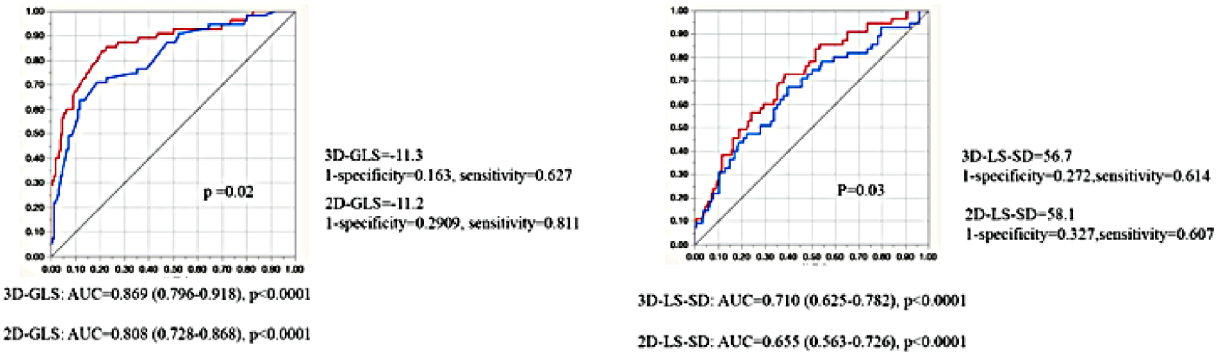

Fig. 1. Receiver operating characteristics curves for predicting MACE. Left, 3D-GLS and 2D-GLS; right. 3D-LS-SD and 2D—LS-SD. These figures show the calculation of receiver operating characteristic (ROC) curves to determine the appropriate cut-off values revealed values. 3D-GLS: AUC = 0.869 (0.796–0.918), p < 0.0001, The optimal cut-off point of 3D-GLS was −11.3 (1-specificity = 0.163, sensitivity = 0.627). 2D-GLS: AUC = 0.808 (0.728–0.868), p < 0.0001. The optimal cut-off point of 2D-GLS was −11.2 (1-specificity = 0.2909, sensitivity = 0.811) 3D-LS-SD: AUC = 0.710 (0.625–0.782), p < 0.0001. The optimal cut-off point of 3D-LS-SD was 56.7 (1-specificity = 0.272, sensitivity = 0.614) 2D-LS-SD: AUC = 0.655 (0.563–0.726), p < 0.0001. The optimal cut-off point of 2D-LS-SD was 58.1(1-specificity = 0.327, sensitivity = 0.607).

Table 2
Univariate and Multivariate Cox proportional hazard models for MACE.

	Univariate			Cox proportional hazard model					
				Using 2D strains indices			Using 3D strain indices		
	HR	(95 %CI)	*p*-value	HR	(95 %CI)	*p*-value	HR	(95 %CI)	*p*-value
Age > 75 years, yes	3.212	(1.831–5.633)	<0.0001	1.91	(1.043–3.831)	0.04	1.925	(1.085–3.413)	0.029
Sex, male, yes	1.481	(0.81–2.732)	0.22	–	–		–	–	
Infarct size > 20%, yes	3.061	(1.791–5.229)	<0.0001	1.28	(0.671–2.456)	0.45	1.4	(0.793–2.472)	0.24
LVEF < 40%	5.177	2.950–9.082	<0.0001	2.019	(1.059–3.842)	0.03	1.933	(1.031–3.651)	0.04
2D-GLS > -11.2%	8.213	(4.494–15.011)	<0.0001	5.947	(3.037–11.631)	<0.0001	–	–	
2D-LS-SD > 58.1msec	2.871	(1.615–5.10)	0.0002	1.577	(0.815–3.042)	0.176	–	–	
3D-GLS > -11.3%	12.558	(6.412–24.563)	<0.0001	–	–		10.656	(4.031–17.131)	<0.0001
3D-LS-SD > 56.7msec	3.762	(2.069–6.832)	<0.0001	–	–		1.991	(1.033–3.613)	0.03

MACE: major adverse cardiac event; HR: hazard ratio; CI: confidence interval.
Abbreviations are described as Table 1.

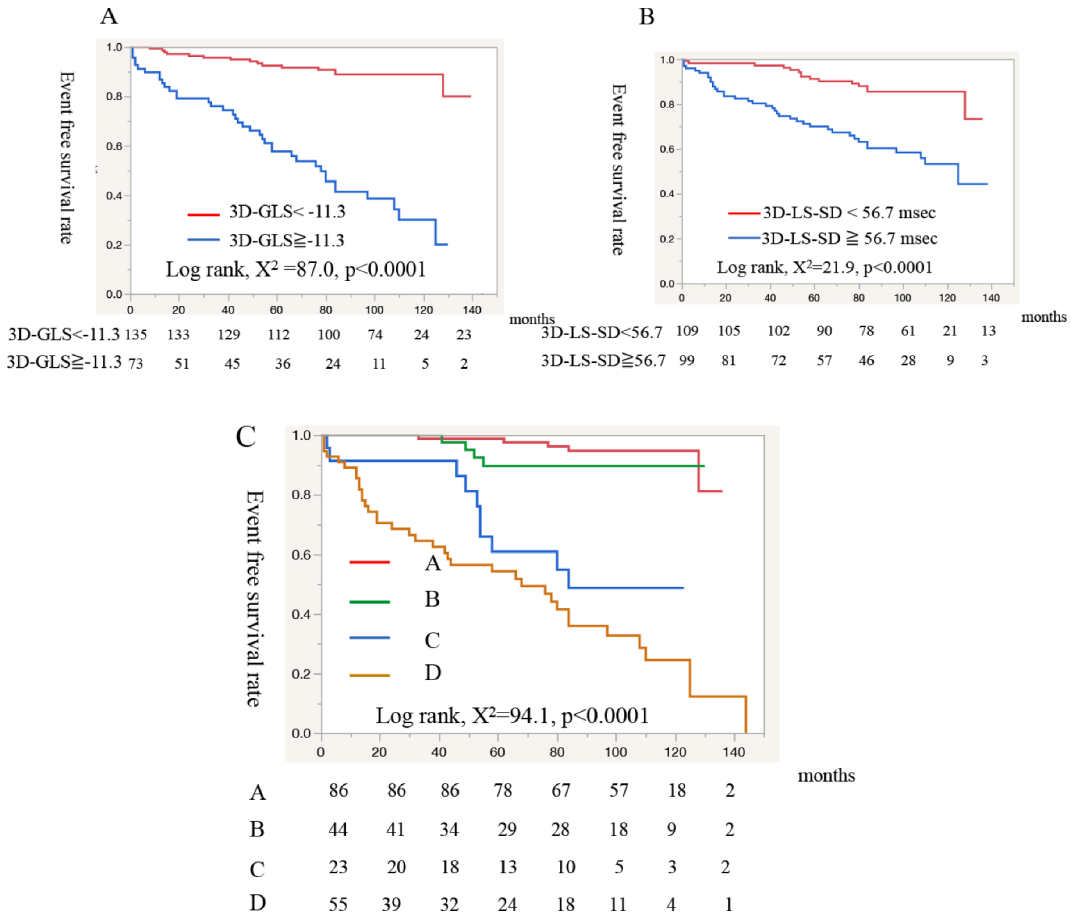

Fig. 2. Kaplan-Meier survival curve analysis for MACE. Fig. 2A shows the significant difference between the patients with 3D-GLS < -11.3 and ≧-11.3(log rank, $\chi^2 = 87.0$, $p < 0.0001$). Fig. 2B shows the significant difference between the patients with 3D-LS-SD < 56.7 ms and ≧56.7 ms(log rank, $\chi^2 = 21.9$, $p < 0.0001$). Fig. 2C shows that of four groups; GroupA: 3D-GLS < -11.3 and 3D-LS-SD < 56.7 ms, GroupB: 3D-GLS≧-11.3 and 3D-LS-SD < 56.7 ms, GroupC: 3D-GLS < -11.3 and 3D-LS-SD≧56.7 ms, GroupD: GLS≧-11.3 and 3D-LS-SD≧56.7 ms. (log rank,$\chi^2 = 94.1$, $p < 0.0001$).

work, thereby potentially impairing functional recovery after myocardial damage.[20] Furthermore, the clinical importance of LV dispersion after AMI has been mainly investigated in relation to LV remodeling, which is a well-known surrogate marker of adverse outcomes [6]. Therefore, LV dispersion can cause substantial LV inefficiencies. Accordingly, the mechanical dispersion of STEMI by LV showed a relationship with systolic and diastolic dysfunction. As shown in Supplementary Fig. 3, significant relationships were apparent between mechanical dispersion and several parameters, such as electrical dispersion (QRS duration), infarct size, and systolic and diastolic function (GLS and E/e'), which are strong independent predictors of outcome in HF.[21–24] Zhang et al. performed sequential echocardiography and contrast-enhanced magnetic resonance imaging (MRI) after AMI and confirmed the relationship between mechanical dispersion and remodeling. [25] The present study verifies recent reports regarding the clinical usefulness of LV dispersion [9] using both 2D-STE and 3D-STE. Moreover, LV dispersion is significantly associated with sudden cardiac death[26]. Therefore, we believe that LV mechanical dispersion measured by 3D-STE can be a strong predictor for STEMI.

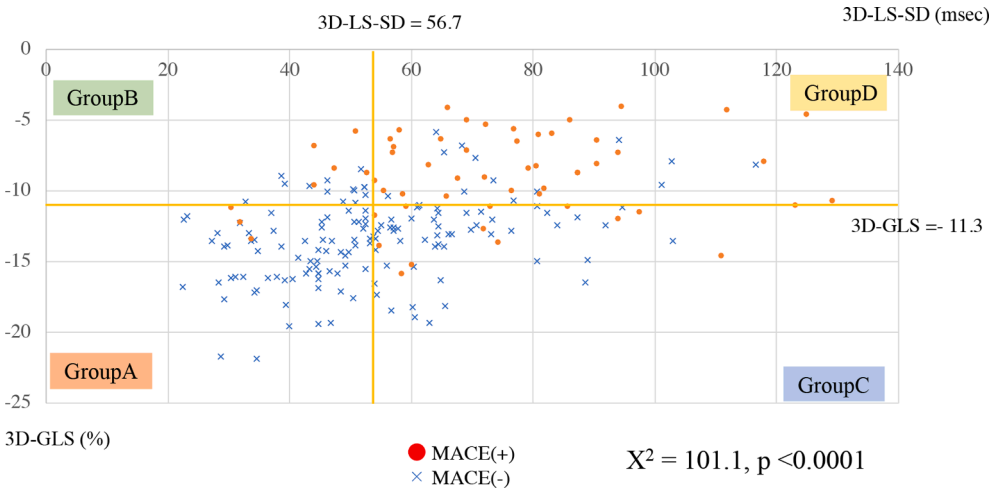

Fig. 3. The plots of 3D-GLS and 3D-LS-SD. Four groups were determined based on the cut-off value determined by the cut-off values of the ROC curves. GroupA: 3D-GLS < -11.3 and 3D-LS-SD < 56.7 msec, GroupB: 3D-GLS≧-11.3 and 3D-LS-SD < 56.7 msec, GroupC: 3D-GLS < -11.3 and 3D-LS-SD≧56.7msec, GroupD: GLS≧-11.3 and 3D-LS-SD≧56.7 msec. The red plot indicates the patients with MACE and the blue plot indicates the patients without MACE. Significant differences among the four groups were observed ($\chi^2 = 101.1$, $p < 0.0001$).

Table 3
Comparison of the hazard risk for MACE among the 4 groups.

	HR	(95 %CI)	*p*-value
Group A	–	–	–
Group B	2.68	0.85–8.41	0.09
Group C	11.75	3.98–34.64	<0.0001
Group D	24.41	18.31–55.62	<0.0001

MACE: major adverse cardiac event; HR: hazard ratio; CI: confidence interval.
Group A: 3D-GLS < -11.3% and 3D-LS-SD < 56.7 ms.
Group B: 3D-GLS≧-11.3 and 3D-LS-SD < 56.7 ms.
Group C: 3D-GLS < -11.3 and 3D-LS-SD≧56.7 ms.
Group D: GLS≧-11.3 and 3D-LS-SD≧56.7 ms.
Abbreviations are described as Table 1.

4.3. Clinical usefulness of three-dimensional speckle tracking

Abou et al. reported the prognostic significance of LV dispersion by 2D-STE in patients with STEMI [9], and their cut-off value (54 ms) was close to that of our obtained value. However, the 2D strain has a through-plane motion problem. For this reason, we view our data as more reliable than previously published results. In fact, 3D data have some advantages over 2D data because of the methodology used for data acquisition[27], which is considered to be one of the greatest merits of 3D-STE.

The 3D nature of 3D-STE technology also provides novel deformation parameters that have the potential to yield a more accurate assessment of overall and regional myocardial function.[28,29] Our previous report on the clinical usefulness of 3D-GLS to predict LV remodeling and the outcomes after the onset of STEMI confirmed the reliability of the 3D-STE modality.[11] Therefore, 3D-STE may represent a rapid method for quantifying global LV mechanical dispersion in patients with STEMI. When compared with the utility of various 3D strain measurements, 3D-STE was superior to 2D-STE.[29] We demonstrated that 3D-STE enables the simultaneous measurement of 3D-GLS and 3D-LS-SD, thereby leading to better determinations of patient prognosis. Our findings showed the usefulness of mechanical dispersion measured by 3D-STE (3D-LS-SD). Therefore, our results can potentially have a great impact on patient prognosis after the onset of STEMI. We believe that the assessment of mechanical dispersion could be a complementary method in 3D-STE, but further verification is required.

4.4. Clinical implications

Our study confirmed that 3D-STE enables the detection of patients at high risk of MACE after the onset of STEMI. The mechanical dispersion estimated by 3D-LS-SD can predict long-term prognosis after STEMI, and a more precise prediction of prognosis after STEMI can be obtained in the acute phase using 3D-STE. The accuracy of prediction is further increased by combining 3D-GLS with 3D-LS-SD, and both indices can be calculated simultaneously. All examinations were performed using 3D-STE as a single-image measurement. The ability to assess patients effectively by simple bedside echocardiographic examinations is the greatest merit of this modality compared to that of the other modalities [30]. We believe that 3D-STE can reveal multidirectional wall motion and LV function, including LV mechanical dispersion, in patients with STEMI.

4.5. Study limitations

This study has several limitations. First, it was a retrospective, single-center study. Second, 2D-STE and 3D-STE were performed using offline software. However, we believe that 3D-STE requires additional progression, which allows easy bedside examination. Third, echocardiographic examinations were performed at the bedside; therefore, scanning the patients was sometimes difficult. We A learning curve was involved, especially in obtaining appropriate data from full-volume 3D images, but the investigators underwent thorough training and careful examination daily. Fourth, the infarct size estimation in all patients was performed by scintigraphy, rather than by MRI and troponin measurements. Recently, late-gadolinium enhancement MRI has been designated as the gold standard for STEMI patients because of its high resolution. However, SPECT can be performed in almost all patients without contraindications.

Fifth limitation was the significant difference among the strain values calculated using different vendor software. [31] For this reason, our analyses were conducted using a vendor-independent software. Sixth, the iE33 instrument is a relatively classical 3D machine; therefore, the volume rate was not high. However, we obtained the highest volume data possible, but this meant excluding patients with a low volume rate from the analysis of mechanical dispersion[32]. Finally, we selected limited indices to analyze with the Cox hazard model because of the limited number of MACEs. There are many significant indices apart from age, gender, infarct size, EF, GLS, and mechanical dispersion. Nevertheless, these limitations may be considered minor, and this newly developed method for the entire LV wall definitely improves the treatment options for cardiac patients.

5. Conclusions

Our study shows that 3D speckle tracking is a useful tool in the predicting long-term prognosis in patients with STEMI who have

undergone reperfusion therapy. We recommend 3D-STE in patients with STEMI because this modality facilitates the examination of both longitudinal wall motion and mechanical dispersion by strain curves and allows simultaneous estimation of both indices. Further studies are needed to confirm the usefulness of 3D-STE in determining the prognosis of STEMI.

Declaration of Competing Interest

The authors declare that they have no known competing financial interests or personal relationships that could have appeared to influence the work reported in this paper.

Acknowledgements

Not applicable

Sources of Funding

Not applicable

Disclosures

Not applicable

Appendix A. Supplementary material

Supplementary data to this article can be found online at https://doi.org/10.1016/j.ijcha.2022.101028.

References

[1] T. Biering-Sørensen, S.J. Shah, I. Anand, N. Sweitzer, B. Claggett, L.i. Liu, B. Pitt, M. A. Pfeffer, S.D. Solomon, A.M. Shah, Prognostic importance of left ventricular mechanical dyssynchrony in heart failure with preserved ejection fraction, Eur. J. Heart Fail. 19 (8) (2017) 1043–1052.

[2] S.-H. Shin, C.-L. Hung, H. Uno, A.H. Hassanein, A. Verma, M. Bourgoun, L. Køber, J.K. Ghali, E.J. Velazquez, R.M. Califf, M.A. Pfeffer, S.D. Solomon, Mechanical dyssynchrony after myocardial infarction in patients with left ventricular dysfunction, heart failure, or both, Circulation 121 (9) (2010) 1096–1103.

[3] I. Kosmidou, B. Redfors, H.P. Selker, H. Thiele, M.R. Patel, J.E. Udelson, et al., Infarct size, left ventricular function, and prognosis in women compared to men after primary percutaneous coronary intervention in ST-segment elevation myocardial infarction: results from an individual patient-level pooled analysis of 10 randomized trials, Eur. Heart J. 38 (2017) 1656–1663.

[4] L.C.R. Hensen, K. Goossens, T. Podlesnikar, J.I. Rotmans, J.W. Jukema, V. Delgado, et al., Left Ventricular Mechanical Dispersion and Global Longitudinal Strain and Ventricular Arrhythmias in Predialysis and Dialysis Patients, J. Am. Soc. Echocardiog.: Official Publication Am. Soc. Echocardiog. 31 (2018) 777–783.

[5] M.G.S.J. Sutton, N. Sharpe, Left ventricular remodeling after myocardial infarction: pathophysiology and therapy, Circulation 101 (25) (2000) 2981–2988.

[6] S.A. Mollema, S.S. Liem, M.S. Suffoletto, G.B. Bleeker, B.L. van der Hoeven, N. R. van de Veire, E. Boersma, E.R. Holman, E.E. van der Wall, M.J. Schalij, J. Gorcsan, J.J. Bax, Left ventricular dyssynchrony acutely after myocardial infarction predicts left ventricular remodeling, J. Am. Coll. Cardiol. 50 (16) (2007) 1532–1540.

[7] M.L. Antoni, H. Boden, G.E. Hoogslag, S.H. Ewe, D. Auger, E.R. Holman, E.E. van der Wall, M.J. Schalij, J.J. Bax, V. Delgado, Prevalence of dyssynchrony and relation with long-term outcome in patients after acute myocardial infarction, Am. J. Cardiol. 108 (12) (2011) 1689–1696.

[8] K.H. Haugaa, B.L. Grenne, C.H. Eek, M. Ersbøll, N. Valeur, J.H. Svendsen, A. Florian, B. Sjøli, H. Brunvand, L. Køber, J.-U. Voigt, W. Desmet, O.A. Smiseth, T. Edvardsen, Strain echocardiography improves risk prediction of ventricular arrhythmias after myocardial infarction, JACC Cardiovasc. Imaging 6 (8) (2013) 841–850.

[9] R. Abou, L. Goedemans, P. van der Bijl, F. Fortuni, E.A. Prihadi, B. Mertens, M. J. Schalij, N. Ajmone Marsan, J.J. Bax, V. Delgado, Correlates and Long-Term Implications of Left Ventricular Mechanical Dispersion by Two-Dimensional Speckle-Tracking Echocardiography in Patients with ST-Segment Elevation Myocardial Infarction, J. Am. Soc. Echocardiog.: Official Publication Am. Soc. Echocardiog. 33 (8) (2020) 964–972.

[10] B.C.F. Smith, G. Dobson, D. Dawson, A. Charalampopoulos, J. Grapsa, P. Nihoyannopoulos, Three-dimensional speckle tracking of the right ventricle: toward optimal quantification of right ventricular dysfunction in pulmonary hypertension, J. Am. Coll. Cardiol. 64 (1) (2014) 41–51.

[11] N. Iwahashi, J. Kirigaya, T. Abe, M. Horii, N. Toya, Y. Hanajima, et al., Impact of three-dimensional global longitudinal strain for patients with acute myocardial infarction, Eur. Heart J. Cardiovasc. Imaging 22 (2020) 1413–1424.

[12] N. Iwahashi, J. Kirigaya, M. Gohbara, T. Abe, M. Horii, Y. Hanajima, N. Toya, H. Takahashi, Y. Minamimoto, Y. Kimura, E. Akiyama, K. Okada, Y. Matsuzawa, N. Maejima, K. Hibi, M. Kosuge, T. Ebina, K. Tamura, K. Kimura, Global Strain Measured by Three-Dimensional Speckle Tracking Echocardiography Is a Useful Predictor for 10-Year Prognosis After a First ST-Elevation Acute Myocardial Infarction, Circulation J.: Official J. Japanese Circulation Soc. 85 (10) (2021) 1735–1743.

[13] R.M. Lang, L.P. Badano, W. Tsang, D.H. Adams, E. Agricola, T. Buck, F.F. Faletra, A. Franke, J. Hung, L. Pérez de Isla, O. Kamp, J.D. Kasprzak, P. Lancellotti, T. H. Marwick, M.L. McCulloch, M.J. Monaghan, P. Nihoyannopoulos, N.G. Pandian, P.A. Pellikka, M. Pepi, D.A. Roberson, S.K. Shernan, G.S. Shirali, L. Sugeng, F. J. Ten Cate, M.A. Vannan, J.L. Zamorano, W.A. Zoghbi, EAE/ASE recommendations for image acquisition and display using three-dimensional echocardiography, J. Am. Soc. Echocardiog.: Official Publication Am. Soc. Echocardiog. 25 (1) (2012) 3–46.

[14] P. Collier, D. Phelan, A. Klein, A Test in Context: Myocardial Strain Measured by Speckle-Tracking Echocardiography, J. Am. Coll. Cardiol. 69 (8) (2017) 1043–1056.

[15] G. Pedrizzetti, S. Sengupta, G. Caracciolo, C.S. Park, M. Amaki, G. Goliasch, et al., Three-dimensional principal strain analysis for characterizing subclinical changes in left ventricular function, J. Am. Soc. Echocardiog.: Official Publication Am. Soc. Echocardiog. 27 (2014) 1041–1050.e1.

[16] J.M. Bland, D.G. Altman, Statistical methods for assessing agreement between two methods of clinical measurement, Lancet (London, England). 1 (1986) 307–310.

[17] M. Takeuchi, K. Fujitani, K. Kurogane, H.-T. Bai, C. Toda, T. Yamasaki, H. Fukuzaki, Effects of left ventricular asynchrony on time constant and extrapolated pressure of left ventricular pressure decay in coronary artery disease, J. Am. Coll. Cardiol. 6 (3) (1985) 597–602.

[18] M. Penicka, J. Bartunek, O. Lang, K. Medilek, P. Tousek, M. Vanderheyden, B. De Bruyne, M. Maruskova, P. Widimsky, Severe left ventricular dyssynchrony is associated with poor prognosis in patients with moderate systolic heart failure undergoing coronary artery bypass grafting, J. Am. Coll. Cardiol. 50 (14) (2007) 1315–1323.

[19] M. Nahlawi, M. Waligora, S.M. Spies, R.O. Bonow, A.H. Kadish, J.J. Goldberger, Left ventricular function during and after right ventricular pacing, J. Am. Coll. Cardiol. 44 (9) (2004) 1883–1888.

[20] C.W. Lewis, C.H. Owen, D.A. Zipprich, D.C. Sabiston, P.K. Smith, D.D. Glower, The effects of local ventricular pacing on recovery from regional myocardial ischemia, J. Surg. Res. 54 (4) (1993) 360–367.

[21] J. Joseph, B.C. Claggett, I.S. Anand, J.L. Fleg, T. Huynh, A.S. Desai, S.D. Solomon, E. O'Meara, S. Mckinlay, B. Pitt, M.A. Pfeffer, E.F. Lewis, QRS Duration Is a Predictor of Adverse Outcomes in Heart Failure With Preserved Ejection Fraction, JACC Heart Fail. 4 (6) (2016) 477–486.

[22] A.M. Shah, S.J. Shah, I.S. Anand, N.K. Sweitzer, E. O'Meara, J.F. Heitner, G. Sopko, G. Li, S.F. Assmann, S.M. McKinlay, B. Pitt, M.A. Pfeffer, S.D. Solomon, Cardiac structure and function in heart failure with preserved ejection fraction: baseline findings from the echocardiographic study of the Treatment of Preserved Cardiac Function Heart Failure with an Aldosterone Antagonist trial, Circulation Heart Fail. 7 (1) (2014) 104–115.

[23] A.M. Shah, B. Claggett, N.K. Sweitzer, S.J. Shah, I.S. Anand, L.i. Liu, B. Pitt, M. A. Pfeffer, S.D. Solomon, Prognostic Importance of Impaired Systolic Function in Heart Failure With Preserved Ejection Fraction and the Impact of Spironolactone, Circulation 132 (5) (2015) 402–414.

[24] E. Donal, L.H. Lund, E. Oger, C. Hage, H. Persson, A. Reynaud, P.-V. Ennezat, F. Bauer, E. Drouet, C. Linde, C. Daubert, New echocardiographic predictors of clinical outcome in patients presenting with heart failure and a preserved left ventricular ejection fraction: a subanalysis of the Ka (Karolinska) Ren (Rennes) Study, Eur. J. Heart Fail. 17 (7) (2015) 680–688.

[25] Y. Zhang, G.W. Yip, A.K.Y. Chan, M. Wang, W.W.M. Lam, J.W.H. Fung, J.Y. S. Chan, J.E. Sanderson, C.-M. Yu, Left ventricular systolic dyssynchrony is a predictor of cardiac remodeling after myocardial infarction, Am. Heart J. 156 (6) (2008) 1124–1132.

[26] R. Perry, S. Patil, C. Marx, M. Horsfall, D.P. Chew, K. Sree Raman, N.D.M. Daril, K. Tiver, M.X. Joseph, A.N. Ganesan, A. McGavigan, G. Nucifora, J. B. Selvanayagam, Advanced Echocardiographic Imaging for Prediction of SCD in Moderate and Severe LV Systolic Function, JACC Cardiovasc. Imaging 13 (2) (2020) 604–612.

[27] S.F. Nagueh, Imaging mechanical dyssynchrony with 3-dimensional echocardiography: a promise still to be fulfilled, JACC Cardiovasc. Imaging 2 (7) (2009) 813–815.

[28] Y. Seo, T. Ishizu, A. Atsumi, R. Kawamura, K. Aonuma, Three-dimensional speckle tracking echocardiography, Circulation J.: Official J. Japanese Circulation Soc. 78 (6) (2014) 1290–1301.

[29] C. Thebault, E. Donal, A. Bernard, O. Moreau, F. Schnell, P. Mabo, C. Leclercq, Real-time three-dimensional speckle tracking echocardiography: a novel technique to quantify global left ventricular mechanical dyssynchrony, Eur. J. Echocardiog.: The J. Working Group Echocardiog. Eur. Soc. Cardiol. 12 (1) (2011) 26–32.

[30] H. Vágó, L. Szabó, Z. Dohy, C. Czimbalmos, A. Tóth, F.I. Suhai, G. Bárczi, V. A. Gyarmathy, D. Becker, B. Merkely, Early cardiac magnetic resonance imaging in

troponin-positive acute chest pain and non-obstructed coronary arteries, Heart (British Cardiac Society). 106 (13) (2020) 992–1000.

[31] L.P. Badano, U. Cucchini, D. Muraru, O. Al Nono, C. Sarais, S. Iliceto, Use of three-dimensional speckle tracking to assess left ventricular myocardial mechanics: inter-vendor consistency and reproducibility of strain measurements, Eur. Heart J. Cardiovasc. Imaging 14 (3) (2013) 285–293.

[32] S. Caselli, F.M. Di Paolo, C. Pisicchio, R. Di Pietro, F.M. Quattrini, B. Di Giacinto, F. Culasso, A. Pelliccia, Three-dimensional echocardiographic characterization of left ventricular remodeling in Olympic athletes, Am. J. Cardiol. 108 (1) (2011) 141–147.